Comparison between three static mixers for emulsification in turbulent flow

F. Theron *, N. Le Sauze

Laboratoire de Génie Chimique, Université de Toulouse, 4 Allée Emile Monso, BP 44 362, 31030 Toulouse Cedex 4, France

A B S T R A C T

This paper deals with comparing performances of three different static mixers in terms of pressure drop generated by both single-phase flow and liquid–liquid flow in turbulent flow regime and in terms of emulsification performances. The three motionless mixers compared are the well-known SMX™ and SMV™ and the new version of the SMX called SMXPlus™. This experimental study aims at highlighting the influence of the dispersed phase concentration and some of the geometrical parameters such as number of elements and design of the motionless mixer on droplets size distributions characteristics. Finally, experimental results are correlated in terms of Sauter mean diameter as a function of hydrodynamic dimensionless numbers.

1. Introduction

Nowadays emulsions have a very large applications range. In fact they may be found as consumable goods such as cosmetic creams, food products like butter or ice creams, or road cover as bitumen emulsions. Moreover emulsions may intervene during processes as a non-wished phenomenon like during oil drilling or as requisite process step. In that case emulsions exhibit some interests like thermal control of exothermic reactions, or size control of final products. In the last case each emulsion droplet may be considered as a reactor where a reaction takes place. In the particular example of microencapsulation by interfacial polycondensation, the polymerization reaction takes place only at droplets interface in order to obtain a particular core shell system.

For most of these applications, it is important to be able to well control the influence of process parameters on droplet size distribution. The particular emulsification device investigated here is the static mixer that enables to work continuously. Static mixers consist in motionless structured inserts called elements placed in cylindrical pipes. These elements induce complex flow fields by redistributing fluids in the directions transverse to the main flow. Mixing elements are placed in series inside the pipe with a 90° rotation between two successive elements. The number of elements can be adjusted. The flow field depends on the mixer design that must be chosen according to the specific mixing operation to carry out and the flow regime.

Static mixers main principles are well described in the open literature (Grace, 1971; Mutsakis et al., 1986; Cybulski and Werner, 1986; Myers et al., 1997; Thakur et al., 2003). They may be used in order to carry out every mixing operation such as mixing of miscible fluids, heat transfer and thermal homogenization, or liquid–liquid dispersion as well as gas–liquid dispersion. Static mixers offers advantages such as no moving parts, small space requirements, little or no maintenance requirements, many construction materials, narrow residence time distributions, enhanced heat transfer, and low power requirements. In fact the only energy cost represented by motionless mixers comes from the external pumping power needed to propel materials through the mixer. That is why their use for continuous processes is an attractive alternative to classical agitation devices since similar and sometimes better performances can be achieved at lower cost.

If static mixers find many industrial applications for mixing of miscible liquids, there are few examples of emulsification with static mixers. The most investigated mixer for liquid–liquid dispersion in turbulent flow in the literature is the classical Kenics helical mixer (Middleman, 1974; Chen and Libby, 1978; Haas, 1987; Berkman and Calabrese, 1988 and Yamamoto et al., 2007). Emulsification using the Sulzer SMX mixer has been studied not only in laminar flow (Legrand et al., 2001; Das et al., 2005; Liu et al., 2005; Rama Rao et al., 2007; Fradette et al., 2007; Gingras et al., 2007) but also in turbulent regime (Streiff et al., 1997). Results about liquid–liquid dispersion are also reported in the literature using the SMV mixer (Streiff, 1977; Streiff et al., 1997), the Lightnin Series 50 (Al Taweel and Walker, 1983; El Hamouz et al., 1994) and the High Efficiency Vortex mixer (Lemenand et al., 2001, 2003, 2005).

If there are a lot of mixer designs commercialised, there are only few available data that enable one to choose the best fitting model according to the flow regime concerned and mostly to the expected sizes. Moreover there is no available energy consumption comparison between different mixers for a given size range. That is why

* Corresponding author.
E-mail address: felicie.theron@ensiacet.fr (F. Theron).

the aim of the present study is to compare the performances of three different Sulzer mixers for emulsification in turbulent flow of the same water/oil/surfactant system. The three mixers tested are the SMX, the SMV and the new SMX plus mixers. If there are still available data about emulsification using the SMX mixer, there are few studies concerning the SMV mixer. The SMX plus mixer is a new modified version of the well-known SMX mixer. The main modification brought to the SMX mixer is the appearance of gap between crossbars. This mixer has been investigated through CFD analysis and LIF measurements by Hirschberg et al. (2009) in order to investigate mixing and residence time distribution performances. One of the intents of the present work is to compare the emulsification performances of this new SMX design to those of both SMX and SMV.

The first part of this paper deals with the hydrodynamic characterization of the three mixers through pressure drops measurements. This enables to highlight the turbulent flow for each mixer and to correlate pressure drops in terms of dimensionless numbers taking into account some geometric parameters of the mixers. Then pressure drops generated by liquid–liquid flow through the mixers are also measured and correlated. About liquid–liquid dispersion the influence of the dispersed phase concentration on droplets size distributions is evaluated for the SMX mixer for rather dilute to concentrate system. The influence of the mixer number of elements and of the mixer design on emulsification's performances is also discussed. Finally Sauter mean diameters obtained for the three mixers are correlated as a function of hydrodynamics dimensionless numbers.

2. Experimental

2.1. Materials

The fluids involved in emulsification experiments were the 1.5 vol.% Tween 80 water solution as continuous phase and cyclohexane as dispersed phase. This concentration, which corresponds to 1.23×10^{-2} mol/L, is much higher than the critical micellar concentration (CMC) of Tween80 whose value has been measured and is 1.2×10^{-5} mol/L. Physico-chemical properties of fluids used are specified in Table 1. The interfacial tension between these two immiscible fluids was measured using the pendant drop method with the Krüss DSA100 tensiometer.

2.2. Static mixers studied

The three static mixers investigated in the present study are commercialized by the Sulzer Company. Pictures of these mixers are presented in Fig. 1 and their geometric characteristics are detailed in Table 2. A 10 mm nominal diameter has been selected in order to limit board effects while limiting material consumptions induced by working in turbulent regime. In Fig. 1 can be seen the gap between crossbars introduced in the original SMX to obtain the new SMX plus. SMX and SMX plus mixers used have the same crossbars number.

2.3. Pressure drop acquisition and emulsification procedure

Fig. 2 is a schematic drawing of the experimental rig used for pressure drop measurements and emulsification. Static mixer elements are inserted into a stainless steel pipe which length enables to work with 20 elements maximum. Pressure drop is measured with a differential pressure sensor. For emulsification the dispersed phase enters the mixer through a small tube of 4 mm inner diameter.

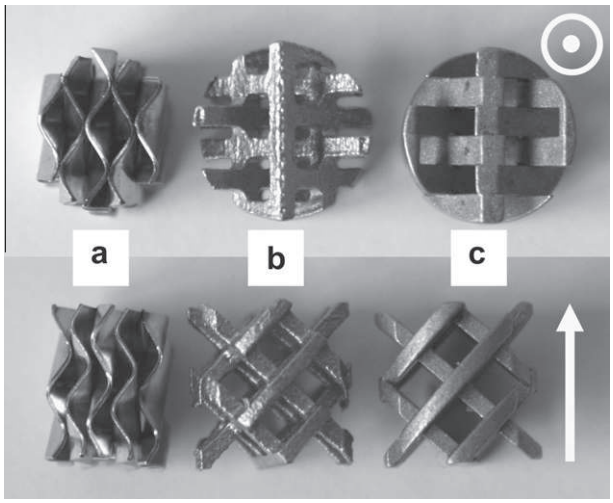

Fig. 1. Pictures of the three mixers used: (a) SMV; (b) SMX plus; and (c) SMX.

2.4. Droplet size distribution analysis

During emulsification experiments droplet size distribution analysis were carried out using a Malvern Mastersizer 2000 (Malvern Instruments). For each analysis a sample of emulsion was diluted in distilled water in order to respect the obscuration range fixed by the apparatus.

3. Results and discussion

3.1. Turbulent flow characterization through single-phase flow pressure drop measurements

Static mixers exhibit numerous advantages relatively to stirred tank for many mixing operations. However they generate high pressure drops directly related to the mixer design that determines the energy cost of the operation. In fact the mean energy dissipation rate can be calculated from measured pressure drops. That is why a compromise must be done between the aim in terms of mixing performances and pressure drops generated.

There are numerous correlations in the open literature that predict pressure drops generated by classical motionless mixers such as Kenics, SMX, etc. These correlations are generally developed for a given flow regime: laminar or turbulent. But for most of these correlations a lack of mixer's geometric characteristics data makes them hardly applicable. That is why the hydrodynamic for the turbulent flow in the three static mixers investigated here has been characterized by the pressure drops generated in single-phase flow, in terms of dimensionless numbers taking into consideration geometric characteristics of mixers that are easy to obtain and that will be specified here.

Table 1
Physico-chemical properties of fluids used.

	Water–glycerol (60 wt.%)	Water–glycerol (40 wt.%)	Cyclohexane	Water–Tween 80 (1.5 vol.%)
Density (kg m^{-3})	1143	1090	770	995
Viscosity (Pa s)	0.0083	0.0032	0.0009	0.0010

Table 2
Geometric characteristics of the three different mixers used.

Mixer's design	SMX	SMX+	SMV
D (mm)	10.15	10.30	9.45
H/D	≈1	≈1	≈1
D_h (mm)	2.45	2.1	3.5
ε	0.67	0.84	0.83
Crossbars number (for SMX and SMX+) or corrugated plates number (SMV)	6	6	5
Crossbars (for SMX and SMX+) or corrugated plates (for SMV) thickness	0.99	1.10	0.14

3.1.1. Highlighting of turbulent flow

Before correlating pressure drops generated by the three motionless mixers the beginning of turbulent flow has been detected based on a dimensionless representation of pressure drops in terms of friction factor as a function of Reynolds number. As for flows in empty pipes the beginning of the turbulent flow may be detected through a curve profile change.

For each design tested pressure drops have been measured for three different mixing elements numbers: $n_e = 5$; 10 and 15. In the literature friction factors f and Reynolds numbers Re are generally calculated as follows, taking into account the superficial velocity V_0 and the mixer diameter D:

$$f = \frac{\Delta P}{2\rho V_0^2}\frac{D}{L} \tag{1}$$

$$\mathrm{Re} = \frac{\rho V_0 D}{\mu} \tag{2}$$

where μ and ρ are respectively the fluid viscosity and density, and L is the mixer length.

Pressure drops obtained in the present study are presented in terms of hydraulic friction factor f_h and Reynolds Re_h taking into account the interstitial velocity V_0/ε and the mixer hydraulic diameter D_h as proposed by Streiff (1999), ε being the mixer's porosity. This representation enables to set free from some geometric characteristics of the mixer.

$$f_h = \frac{\Delta P \varepsilon^2}{2\rho V_0^2}\frac{D_h}{L} \tag{3}$$

$$\mathrm{Re}_h = \frac{\rho V_0 D_h}{\varepsilon \mu} \tag{4}$$

Experimental data are presented in Figs. 3–5. These figures show that for each mixer friction factors obtained are higher for five elements than for 10 and 15 elements. This phenomenon comes from higher linear pressure drops $\Delta P/L$. This linear pressure drop decrease with n_e is never mentioned in the literature. In fact it is generally admitted that linear pressure drops are constants along the mixer, as shown by Karoui (1998) who worked with a 50 mm SMV mixer with $n_e = 1$; 2 and 3, and insisted on the fact that there is no pressure drop creation at the interface between two successive mixers. For the present experimental rig that involves 10 mm diameter mixers there might be an entrance effect du to turbulent eddies generating a singular pressure drop. This entrance effect is here particularly important because of the small

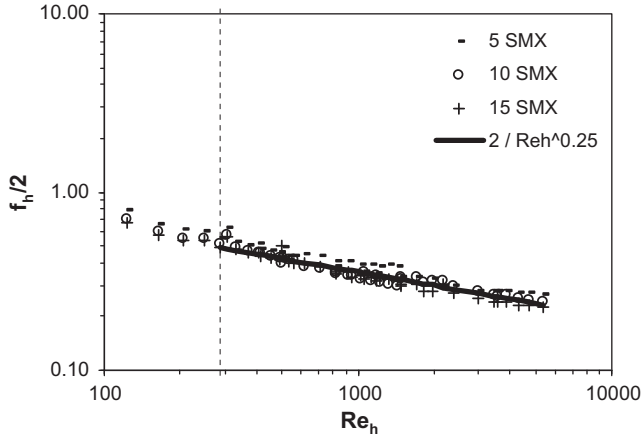

Fig. 3. $f_h/2 = f(\mathrm{Re}_h)$ for the SMX mixer with $n_e = 5$; 10; 15.

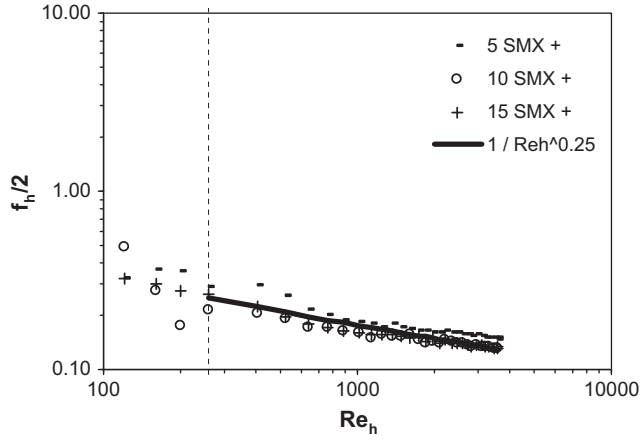

Fig. 4. $f_h/2 = f(\mathrm{Re}_h)$ for the SMX + mixer with $n_e = 5$; 10; 15.

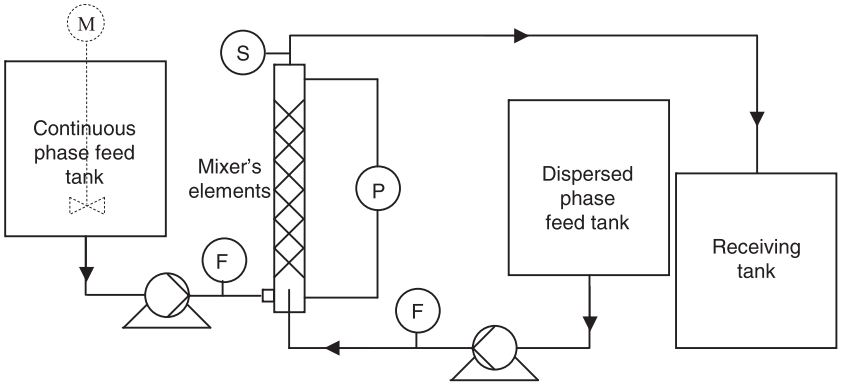

Fig. 2. Schematic diagram of the experimental rig: *F*, flowmeter; *P*: differential pressure sensor; *S*: sampling valve.

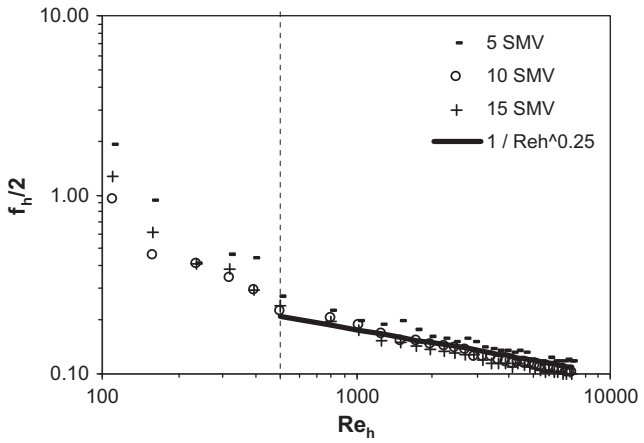

Fig. 5. $f_h/2 = f(\mathrm{Re}_h)$ for the SMV mixer with $n_e = 5; 10; 15$.

diameters of mixers. When the number of mixers increases this singular pressure drop becomes negligible compared to the pressure drop due to the mixers.

Apart from the entrance effect highlighted for $n_e = 5$, the $f_h/2 = f(\mathrm{Re}_h)$ graphs exhibit the same profile for the three mixers. For the SMV, SMX plus and SMX mixers the turbulent flow regime appears respectively at Re_h equals to 500, 260 and 290, what corresponds to Re equals to 1130, 800 and 1060.

It is interesting to notice that turbulent flow is reached for lower Reynolds number for SMX and SMX plus mixers than for the SMV. The representation of experimental data in terms of hydraulic Reynolds number and friction factor enables to set free from two geometric characteristics: porosity and hydraulic diameters. The deviation reported here between the two versions of the SMX mixer and the SMV may be attributed to the intrinsic geometry of both designs. In fact the SMX geometry appears to be a more efficient turbulence promoter than the more "closed design" and smoother SMV.

The Reynolds values characterizing the beginning of the turbulent flow are in quite good agreement with values indicated in the literature. In fact Pahl and Muschelknautz (1980, 1982) set the establishment of the turbulent flow at Re = 1000 for the SMV mixer and the SMX mixer. Li et al. (1996, 1997) also find a Re = 1000 value for the case of the SMX mixer.

3.1.2. Correlation of experimental results and comparison between pressure drops generated by the three mixers

Different correlation types are usually employed to represent pressure drops generated by motionless mixers. A first approach consists in comparing pressure drops generated by static mixers ΔP_{SM} to pressure drops generated by a similar flowrate through an empty pipe with the same diameter as the mixer ΔP_{EP} through the Z factor defined as follows:

$$Z = \frac{\Delta P_{SM}}{\Delta P_{EP}} \tag{5}$$

Table 3
Correlations of pressure drop in SMX mixer from the literature.

Authors	Mixer's characteristics	Correlation	Z	Reynolds range
Pahl and Muschelknautz (1979)	D = 50 mm L_e/D = 1,5 n_e = 5; 7; 9	Z = 10–100	10–100	Re ⩽ 50
Pahl and Muschelknautz (1980, 1982)		Z = 10–60 φ_d = 2, Ne = 12	10–60	Re ⩽ 50 Re > 1000
Alloca (1982)	D = 50 mm L_e/D = 1 n_e = 5, 7, 11 ε = 0.91	Ne·Re = 1237 (Sulzer: Ne·Re = 1200)		
Heywood et al.(1984)	D = 25 mm L_e/D = 1.8 n_e = 4	Z = 18.1 $\zeta = 2.\mathrm{Ne} = \frac{1893}{\mathrm{Re}}$	30	Re = 10^{-4} 1.8 < Re < 20
Bohnet et al. (1990)	D = 50 mm	$\zeta = 2.\mathrm{Ne} = \frac{1740.8}{\mathrm{Re}} + 7.68$ $\zeta = 2.\mathrm{Ne} = \frac{72.7}{\mathrm{Re}^{0.25}}$	230	20 < Re < 850. . .2150 Re < 4000
Shah and Kale (1991, 1992)	D = 26; 54 mm L_e/D = 1.5 n_e = 24 ε = 0.87	$f_i = \frac{350}{\mathrm{Re}_i} + \frac{5.13}{\mathrm{Re}_i^{0.58}}$		Re_i < 10 (≈Re < 10)
Li et al. (1996, 1997)	D = 16 mm L_e/D = 1,25 n_e = 6, 8, 12 ε = 0.84	$\frac{f}{2} = \frac{184}{\mathrm{Re}}$ $\frac{f}{2} = \frac{110}{\mathrm{Re}^{0.8}} + 0.4$ $\frac{f}{2} = \frac{6}{\mathrm{Re}^{0.25}}$	23 152	Re < 15 15 < Re < 1000 1000 < Re < 10,000
Streiff et al. (1999)		$\mathrm{Ne} = \frac{1200}{\mathrm{Re}} + 5$	Z = 38	Laminar: Re_h < 20 Turbulent: Re_h > 2300
Yang and Park (2004)	D = 40 mm L_e/D = 1 n_e = 4, 8, 12	$\frac{f}{2} = \frac{8.55}{\mathrm{Re}^{1.61}}$		Re < 20
Rama Rao et al. (2007)	D = 15.75; 41.18 mm L_e/D = 1 n_e = 6, 8, 10 ε = 0.892; 0.833	D = 15,75 mm $\mathrm{Ne} = \frac{1290}{\mathrm{Re}} + 10.9$ D = 41.78 mm $\mathrm{Ne} = \frac{823}{\mathrm{Re}} + 7.85$		Laminar: Z = 40 Laminar: Z = 26

Table 4
Correlations of pressure drop in SMV mixer from the literature.

Authors	Mixer's characteristics	Correlation	Z	Reynolds range
Pahl and Muschelknautz (1979)	D = 50 mm L_e/D = 1.0 n_e = 2	Z = 65–100	65–100	Re ⩽ 50
Pahl and Muschelknautz (1980, 1982)		φ_d = 2 Ne = 6–12		Re > 1000
Alloca (1982)	D = 50 mm L_e/D = 1.0 n_e = 7, 14 ε = 0.88	Ne·Re = 1430		
Heywood et al. (1984)	D = 25 mm L_e/D = 1.2 n_e = 6	Z = 33.3		Re = 10^{-4}
Karoui (1998)	D = 50 mm L_e/D = 1 n_e = 1, 2, 3 D_h = 9.3 mm ε = 0.74	Ne = 31.06·$Re^{-0.2}$		Re ≈ 2300–60,000
Streiff et al. (1999)		$Ne = \frac{1430}{Re} + 1$ (2)		Laminar: Re_h < 20 Turbulent: Re_h > 2300

This expression is only valid for Newtonian fluids and is determined for each flow regime. This approach is used by Pahl and Muschelknautz (1979, 1980, 1982), Heywood et al. (1984) and Lemenand et al. (2005) who report Z factors for different mixer designs.

Numerous authors chose to treat the whole flow regimes through one equation as follows:

$$\mathrm{Ne} = \frac{C_1}{\mathrm{Re}} + C_2 \tag{6}$$

Where Ne is the Newton number that is similar to the friction factor:

$$\mathrm{Ne} = 2f = \frac{\Delta P}{\rho V_0^2}\frac{D}{L} \tag{7}$$

Some author also used the Newton number or the friction factor but treated separately laminar, transient and turbulent flow. For laminar flow this number is often related to the Reynolds number through correlations similar to Hagen Poiseuille (Bird et al., 1924) correlation, that models pressure drop in laminar flow in empty pipes:

$$\mathrm{Ne} = \frac{C_3}{\mathrm{Re}} \tag{8}$$

This equation enables to predict pressure drops in empty pipes as follows:

$$f = \frac{16}{\mathrm{Re}} \tag{9}$$

This correlation is valid for Re < 2100 and may be used to calculate Z factors in laminar flow.

For turbulent flow the Newton number of the friction factor are related to the Reynolds as follows:

$$\mathrm{Ne} = \frac{C_4}{\mathrm{Re}^{C_5}} \tag{10}$$

Bohnet et al. (1990) and Li et al. (1996, 1997) treated the turbulent flow in SMX mixer through correlations like equation 10, and found a C_5 value of −0.25 which corresponds to the Reynolds exponent of the Blasius (Bird et al., 1924) equation used for empty pipes flows in turbulent regime:

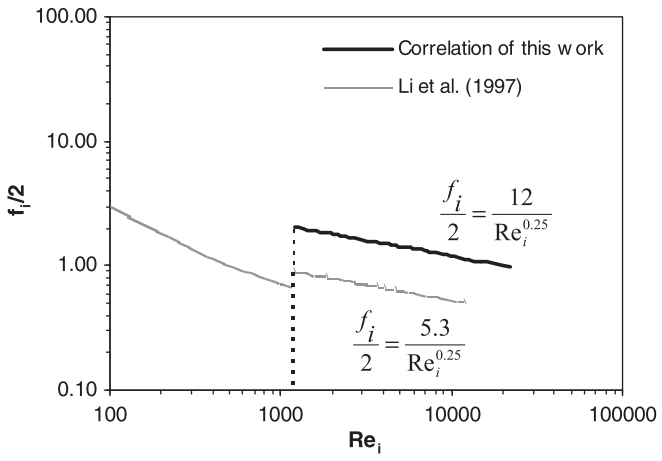

Fig. 6. Comparison between the correlation proposed in this work and Li et al. (1997) correlation for the case of the SMX mixer.

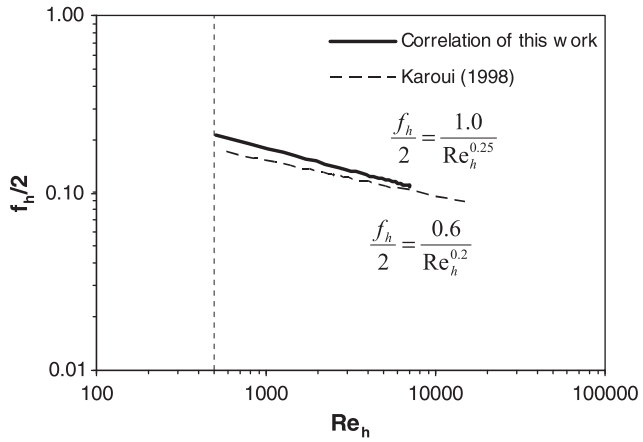

Fig. 7. Comparison between the correlation proposed in this work and Karoui (1998) correlation for the case of the SMV mixer.

$$f = \frac{0.0791}{\mathrm{Re}^{0.25}} \tag{11}$$

This equation which is valid for 2100 < Re < 100,000 also enables to calculate Z factors in turbulent flow.

Finally, in order to treat the transient flow Bohnet et al. (1991) and Li et al. (1996, 1997) proposed correlations of the following form:

$$\mathrm{Ne} = \frac{C_6}{\mathrm{Re}^{C_7}} + C_8 \tag{12}$$

Correlations of the literature for respectively SMX and SMV mixers are recapitulated in Tables 3 and 4. The new SMX plus static mixer tested here is rather recent, so there are no experimental data available that deals with pressure drops. Performances of this mixer in terms of pressure drops, mixing and residence time distribution have been evaluated through CFD analysis by Hirschberg et al. (2009). The predicted pressure drops were less than 50% of the pressure drops of the original SMX.

3.1.3. Correlation of experimental results and comparison between pressure drops generated by the three mixers

For the three designs tested experimental data obtained in turbulent regime present a linear profile through a logarithmic representation. This profile type may be correlated through a Blasius type equation as proposed by Bohnet et al. (1991) and Li et al. (1996) for the SMX mixer:

$$f = \frac{C_9}{\mathrm{Re}^{0.25}} \tag{13}$$

where C_9 is a constant.

In order to take into account the geometric characteristics of each mixer tested here hydraulic friction factors and Reynolds numbers are correlated through equations of the following form:

$$\frac{f_h}{2} = \frac{C_{10}}{\mathrm{Re}_h^{0.25}} \tag{14}$$

The profiles obtained are presented in Figs. 3–5.

For each design Blasius type correlations fits well experimental data. The C_{10} numerator value obtained for the SMV and the SMX plus mixers is equal to 1 and is of 2 for the SMX mixer. So pressure drops generated by the SMX plus mixer are similar to those generated by the SMV mixer and are well reduced to 50% compared to its new version. This result is in good agreement with Hirschberg et al. (2009) CFD analysis. It must be highlighted here that the representation in terms of "hydraulic" values enables to detect discrepancies directly due to mixers design.

3.1.4. Comparison to correlations of the literature

It has been pointed out before that factors influencing pressure drops depend not only on mixer's design, but also on its geometric characteristics such as the gap between crossbars for the SMX plus mixer. In order to well compare the results of the present study to the literature, it is necessary to take into account the maximum of geometric characteristics and in particular the porosity and the hydraulic diameter. The mixer's roughness is never mentioned in the literature but it may be considered in the future as was done for correlations dealing with pressure drops in empty pipes.

On Fig. 6 the correlation established in this work for the SMX mixer is compared to the correlation obtained by Li et al. (1997) in terms of interstitial friction factor f_i and Reynolds number Re_i defined by Shah and Kale (1991, 1992). These numbers take into account the mixer's porosity through the interstitial velocity V_0/ε as follows:

$$f_i = \frac{\Delta P \varepsilon^2}{2\rho V_0^2}\frac{D}{L} \tag{15}$$

$$\mathrm{Re}_i = \frac{\rho V_0 D}{\mu \varepsilon} \tag{16}$$

Nevertheless as Li et al. (1997) do not precise the hydraulic diameter of the mixer used this last parameter cannot be taken into consideration.

The porosity cannot explain the whole discrepancy between both correlations treating the turbulent flow but it appears here as an important parameter. In fact the numerators ratio is of about 2 when representing results in terms of interstitial velocity V_0/ε whereas it is of 4 when representing them in terms of superficial velocity V_0. It would have been interesting to know the hydraulic diameter of the mixer used by Li et al. (1997) in order to compare results by introducing geometric parameters into correlations and to evaluate the respective influence of each parameter step by step.

Moreover the SMX mixer used by Li et al. (1997) has a diameter of 15 mm and an aspect ratio $L_e/D = 1.5$ whereas the SMX mixer studied here has a diameter of 10 mm and an aspect ratio $L_e/D = 1.0$. These characteristics may also have an influence on pressure drops. Particularly a smaller mixer diameter may generate a board effect, what could result in higher pressure drops.

About the SMV mixer, the correlation used in the present work to treat the turbulent flow regime is compared in Fig. 7 to the correlation obtained by Karoui (1998) in terms of hydraulic numbers. The results obtained from both studies in a same Reynolds number range are quite similar. In the correlation of pressure drops proposed by Karoui (1998) the exponent of the Reynolds number was not taken equal to −0.25 like in the Blasius law as made in the present work, but was determined and is equal to −0.2. The numerator obtained by Karoui (1998) was of 0.6 whereas it is of 1.0 for the present study.

The small difference between pressure drops measured in both cases may be due to a different mixer diameter. In fact the SMV used by Karoui (1998) has a 50 mm diameter whereas the SMV tested has a 10 mm one. So as mentioned before a smaller mixer diameter may generate a board effect that results in higher pressure drops.

As expected it has been shown here that pressure drops generated by static mixers differ from one mixer to each other. But each static mixer design has many geometric characteristics among which have been pointed out here the diameter, the porosity, the aspect ratio L_e/D and the hydraulic diameter. And these parameters significantly influence pressure drops. For example it has been demonstrated that pressure drops raise when the diameter decreases due to some board effect. Concerning the SMX mixer it has been shown that the introduction of a gap between crossbars enables to reduce pressure drops of about 50%. As a consequence correlations predicting pressure drops generated by static mixers must take into account as much geometric parameters as possible.

Moreover it is possible that some other parameters such as mixer roughness play a role in pressure drops and particularly in turbulent flow regime.

3.2. Pressure drops generated by emulsions

Pressure drops generated by emulsion flows with a 25% dispersed phase concentration in volume through the three mixers are presented in Fig. 8 in terms of hydraulic friction factor as a function of hydraulic Reynolds number. In order to calculate these values the continuous phase properties have been used.

Fig. 8 shows that pressure drops generated by the same liquid–liquid system are about two times higher for the SMX mixer than for the SMX plus and SMV ones. Moreover a Blasius like correlation

fits well with experimental results obtained with the three mixers. Numerators are quite similar for the SMX plus and the SMV mixer. In fact they are respectively of 0.9 and 0.8.

Finally numerators for the diphasic system are almost equals to those obtained for single-phase flow. In fact it is of 2 for the SMX mixer in monophasic and dysphasic cases and it is of about 1 in both cases for the SMX plus and SMV mixers. This result enables to conclude that the apparent viscosity of emulsions is close to the continuous phase one. This phenomenon may be explained by the fact that emulsions prepared here are rather dilute.

3.3. Emulsification

3.3.1. Parameters investigated

Many published study that deal with emulsification in static mixers investigate the influence of physico-chemical parameters such as interfacial tension between the two phases or viscosity ratio on emulsification performances for a given static mixer (Middleman, 1974; Streiff, 1977; Chen and Libby, 1978; Matsumura et al., 1981; Haas, 1987; Berkman and Calabrese, 1988). The main motivation of the present study is to evaluate the impact of geometric parameters of mixers used such as the number of elements and the design of the mixer on the energy cost of the emulsification process.

Table 5 recapitulates experimental conditions carried out for the present study. The influence of the number of mixer elements n_e as well as the total flowrate Q_{tot} was evaluated for each mixer, at a fixed dispersed phase concentration Φ of 25% in volume. For the SMX mixer four different dispersed phase concentrations were tested from dilute to concentrated systems. Experimentally the dispersed phase concentration is fixed through respective flowrates of each phase as follows:

$$\phi = \frac{Q_d}{Q_c + Q_d} \tag{17}$$

where Q_d and Q_c are respectively the dispersed phase and continuous phase flowrates.

Residence times t_r in static mixers resulting from experimental conditions are also precised in Table 5. These values are calculated through the following expression:

$$t_r = \frac{\varepsilon V_{apparent}}{Q_{tot}} \tag{18}$$

where $\varepsilon \cdot V_{apparent}$ is the mixer's volume really offered to the liquid flow taking into consideration the mixer's porosity.

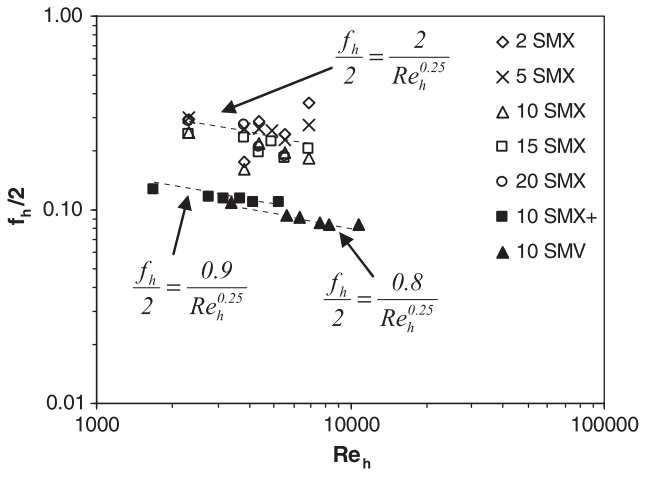

Fig. 8. Comparison between liquid–liquid experimental pressure drops for a 25% dispersed phase concentration in volume and correlations established with single-phase flow results.

3.3.2. Droplets size characterization

Fig. 9 shows an example of optical microscopy picture of emulsion droplets obtained during this study. Droplets are well spherical and their sizes range from about 10 to 70 μm.

Fig. 10 represents the droplets size distribution of an emulsion sample obtained during the same experiment. This distribution is monodisperse and follows a log–normal profile. The Sauter mean diameter D_{32} as well as the SPAN that represents the deviation of the distribution are quantified for each droplets size distribution. These values are defined as follows.

$$D_{32} = \frac{\sum_{i=1}^{n} n_i d_i^3}{\sum_{i=1}^{n} n_i d_i^3} \tag{19}$$

$$\text{SPAN} = \frac{d_{90} - d_{10}}{d_{50}} \tag{20}$$

where d_{90}, d_{10} and d_{50} are characteristic diameters that represent the highest droplets diameter of respectively 90%, 10% and 50% in volume of the dispersed phase.

The Sauter mean diameter of the droplets size distribution represented in Fig. 10 is of 25.2 μm and its SPAN is of 0.98. Moreover droplets sizes range from about 9 to 70 μm what is in good agreement with droplets sizes measured from the optical microscopy picture (Fig. 9).

Every droplets size distributions obtained during this study have the same characteristics as the distribution presented on Fig. 10: monodispersity and of log–normal type.

Finally every emulsion prepared during this study showed a creaming phenomenon noticeable several minutes after the operation. That is why droplet size distribution analysis was repeated about 24 h after emulsification in order to asses the stability of emulsions. Fig. 11 illustrates the comparison between the size distribution just after emulsification and about 24 h after the operation.

Both droplets size distributions in volume presented in Fig. 11 show a similar profile with Sauter mean diameters of about 18 μm. In order to ensure that the minimum size diameter has not change these distributions are presented in Fig. 12 in terms of droplets size distributions in number that focus more on smallest sizes. These distributions also highlight that no irreversible phenomenon like coalescence or Ostwald ripening has occurred.

3.3.3. Influence of the different parameters tested: Φ, n_e, mixer design

3.3.3.1. Influence of the dispersed phase concentration Φ. Most of models of the literature predicting mean droplets size resulting from emulsification in static mixers are only proposed for very dilute systems ($\Phi \leqslant 0.1$). For such concentration ranges there are probably few coalescence effects. Moreover such concentrations do not well represent industrial conditions. That is why some experiments have been carried out with dispersed phase concentrations ranging from 0.1 to 0.6 what enables to include dilute to rather concentrated systems. These experiments have been realized with SMX static mixer made of 10 elements at a total flowrate of 335 L/h. The droplets size distributions obtained for the four different dispersed phase concentrations tested are presented in Fig. 13 and the respective D_{32} and SPAN characterizing each distributions are reported in Table 6.

Fig. 13 shows that the distribution obtained for a rather dilute system ($\Phi = 0.10$) is moved to the left corresponding to the smaller sizes compared to the three other distributions of more concentrated systems. Consequently the minimum, maximum and D_{32} diameters are lower for $\Phi = 0.10$. The sizes distributions corresponding to $\Phi = 0.25$ and $\Phi = 0.40$ are quite similar with $D_{32} \approx 37$ μm, and the one obtained for $\Phi = 0.60$ widens to the highest sizes what results in $D_{32} \approx 40$ μm.

Table 5
Experimental conditions for emulsification experiments.

Mixer's design	Φ	Number of elements n_e	Q_{tot} (L/h)	t_s (s)
SMX	0.1; 0.25; 0.4; 0.6	10	335	
	0.25	2; 5; 10; 15; 20	204; 335; 383; 435; 485; 600	0.10–0.03
SMX +	0.25	2; 5; 10; 15	204; 383; 447; 500; 630	0.10–0.04
SMV	0.25	2; 5; 10; 15; 19	204; 383; 459; 500; 647	0.08–0.04

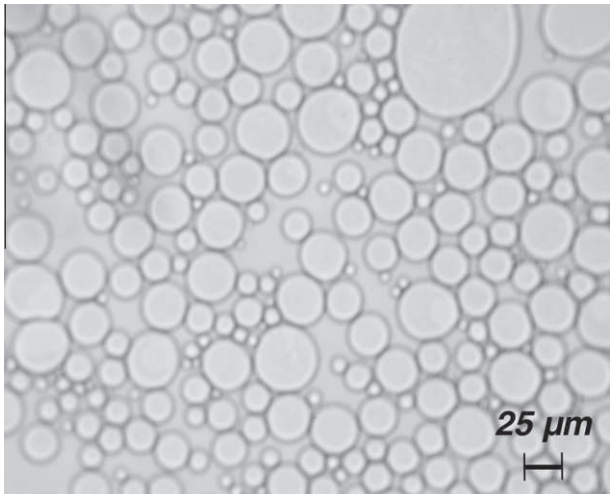

Fig. 9. Optical microscopy picture: SMX mixer; n_e = 10; Q_{tot} = 435 L/h.

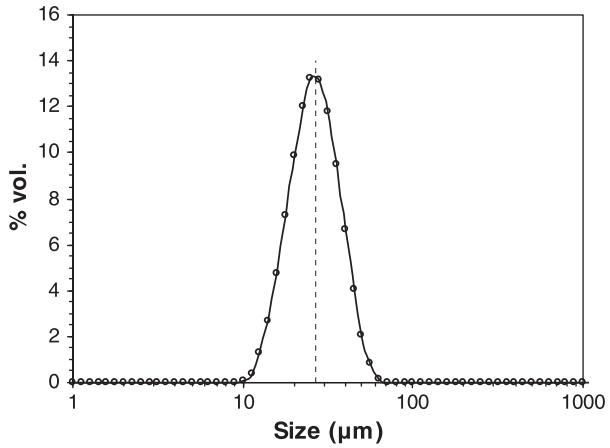

Fig. 10. Droplet size distribution obtained with the SMX mixer with Q_{tot} = 435 L/h and n_e = 10.

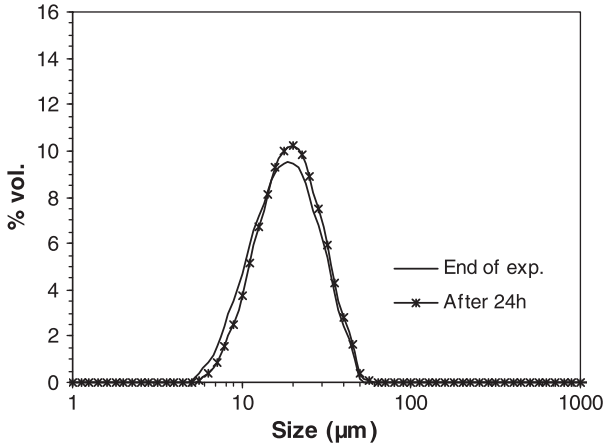

Fig. 11. Volume droplet size distribution obtained after the experiment and about 24 h after the operation with the SMV mixer with Q_{tot} = 500 L/h and n_e = 10.

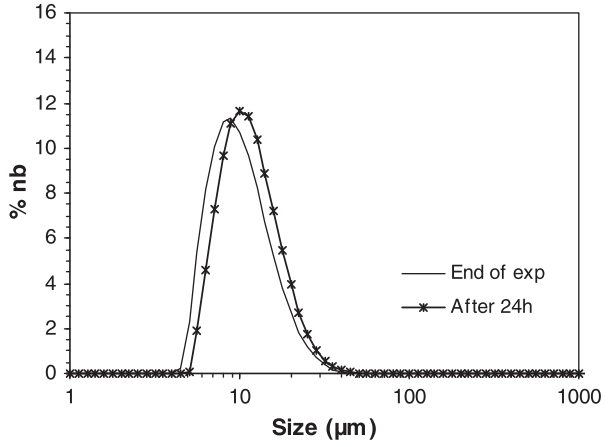

Fig. 12. Number droplet size distribution obtained after the experiment and about 24 h after the operation with the SMV mixer with Q_{tot} = 500 L/h and n_e = 10.

These results indicate that from Φ = 0.25 there is a little influence of the dispersed phase concentration on droplets size distributions obtained, whatever the dispersed phase concentration. This result can be explained by the low residence times in static mixer resulting from total flowrates tested, that may not let enough time for any coalescence phenomenon to occur.

3.3.3.2. Influence of the mixer elements number n_e. In this part of the study the influence of the number of elements, i.e. of the mixer length on the droplets size distribution is evaluated. Note that operating with no element leads to opalescent and unstable emulsions. The droplet sizes range from 10 to 1000 µm (cf. Fig. 14) and distributions are not reproducible, and either mono or polydisperse even measured on a same sample. Consequently in that case, a mean diameter is not appropriate to characterize the emulsion.

The evolution of the Sauter mean diameter D_{32} along the mixer length is presented in Fig. 15 for a total flowrate of 335 L/h, and a dispersed phase concentration of 25% in volume. Fig. 15 shows that the D_{32} decreases as the number of elements increases for each mixer's design. For all mixers D_{32} decreases significantly from 2 to 10 elements and, then tends to level off to an almost constant value for SMV and SMX plus mixers. At this flowrate for the SMX mixer, the stabilization is not satisfactorily obtained with 10 elements. However, a more complete investigation for various flowrates (Theron et al., 2010) has shown that 10 elements are enough to reach the equilibrium droplet size distribution when operating at flowrates higher than 383 L/h.

An explanation of curves profiles presented in Fig. 15 is that in the first 5 elements the biggest droplets are significantly broken, so the break up phenomenon is highly predominant. Then the mean diameter tends to a kind of equilibrium. Each total flowrate

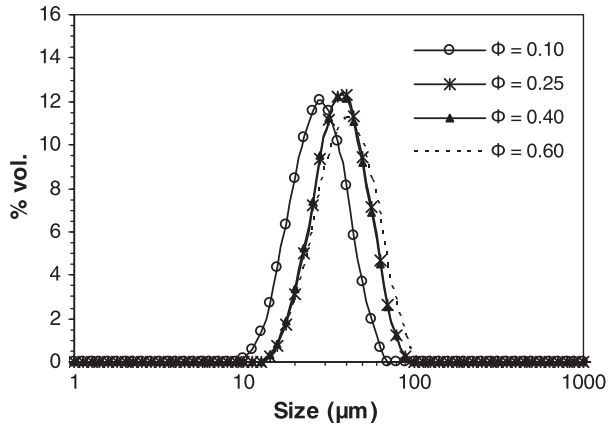

Fig. 13. Influence of the dispersed phase concentration on the droplet size distribution: SMX mixer; $n_e = 10$; $Q_{tot} = 335$ L/h.

Table 6
Sauter mean diameter and SPAN obtained for experiments carried out with the SMX mixer for the different dispersed phase concentrations at $Q_{tot} = 335$ L/h and $n_e = 10$.

Φ	0.10	0.25	0.40	0.60
D_{32} (µm)	27.4	37.2	36.7	40.2
SPAN	0.97	0.92	0.94	1.07

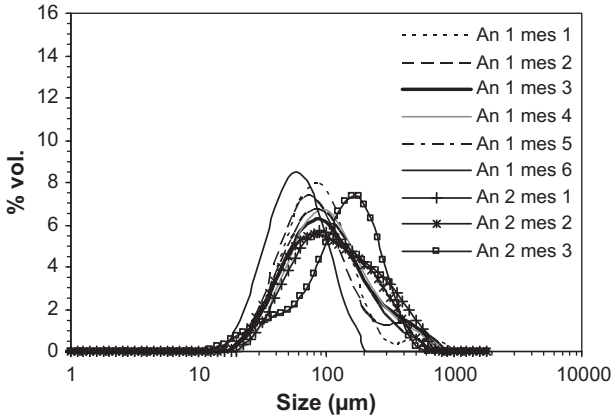

Fig. 14. Droplet size distributions obtained from two analysis of a same experiment obtained when working without any mixing element, with $Q_{tot} = 383$ L/h, and $\Phi = 0.25$.

corresponds to a specific turbulence level what results in different mean diameters at equilibrium. This result is in good agreement with Streiff et al. (1997) observations concerning the SMX and SMV mixers for dilute systems ($\Phi = 0.01$).

The energy cost of the operation is directly related to the pressure drop generated by the emulsion flow across the mixer, which is proportional to the mixer length, i.e. to the number of elements. Our results show that from 10 elements the mean diameter decrease is not significant for the SMV and SMX plus mixers, and small for the SMX. So for every mixer design the use of 10 elements appears to be a good compromise between the energy cost of the operation and the droplets size reached.

3.3.3.3. Influence of the mixer's design. The performances of the three mixer's design are compared in Fig. 16 for a given flowrate ($Q_{tot} = 383$ L/h) and a given dispersed phase concentration ($\Phi = 0.25$). The D_{32} and SPAN values corresponding to each distribution are specified in Table 7. Fig. 16 shows that the narrowest

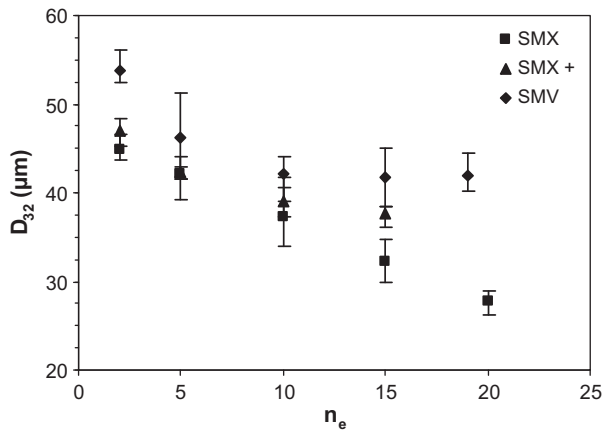

Fig. 15. Influence of the number of elements on the Sauter diameter for the three designs with $Q_{tot} = 335$ L/h.

distribution is obtained when using the SMX mixer, whereas the broadest one is obtained when operating with the SMV mixer. It must be pointed out that the distribution width difference between the three distributions is due to different maximum diameters whereas the three minimum diameters are almost equals.

The minimum diameter is related to the smallest eddies sizes generated by the mixers structures. Those eddies are located close to the tube wall and at mixers baffles intersections (Streiff et al., 1997). This may explain why for a similar total flowrate the same minimum diameter is obtained for the three mixers. But if the SMX and SMX plus mixers have really similar structures, the gap between crossbars certainly induce different repartition and residence time of the fluid in the different shear zones of the mixer. That is surely why different maximum diameters are reached for these two mixers. The same analysis may be done to explain maximum diameter obtained with the SMV mixer which structure concept is really different compared to the two SMX mixers. A local analysis of flows in these mixers would confirm this assumption and explain differences between maximum diameters obtained here.

The three mixers studied generate different pressure drops at a similar flowrate, what results in different mean energy dissipation rates. In order to compare the performances of the three mixers in terms of mean energy dissipation by fluid mass unit ε_m, this value has been calculated from the pressure drops through the following equation:

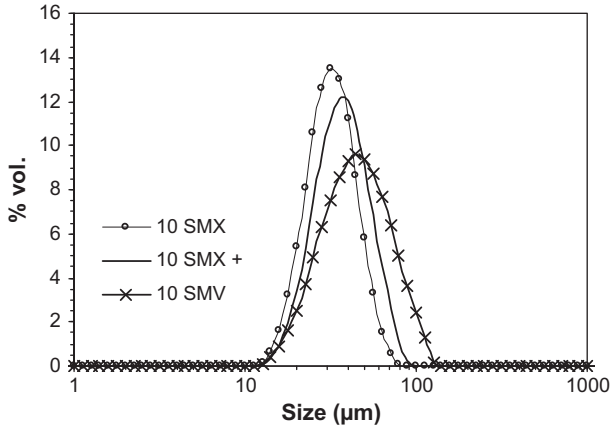

Fig. 16. Comparison of droplet size distributions obtained with the three designs with the same flowrate and the same number of elements: $Q_{tot} = 383$ L/h, $n_e = 10$, and $\Phi = 0.25$.

Table 7
Sauter mean diameter and SPAN obtained bor experiments carried out with the three mixers with Q_{tot} = 383 L/h, n_e = 10 and Φ = 0.25.

Mixer	SMX	SMX+	SMV
D_{32} (μm)	31.8	36.5	46.5
SPAN	0.91	0.95	1.28

$$\varepsilon_m = \frac{Q_{tot}\Delta P}{\varepsilon V_{apparent}\rho_c} = \frac{Q_{tot}\Delta P}{\varepsilon L\frac{\pi D^2}{4}\rho_c} \tag{21}$$

Fig. 17 compares Sauter mean diameters obtained for each mixer at different ε_m. This diagram shows that in the flowrate range studied, for a similar mean energy dissipated the SMV static mixer produces the lowest mean droplets sizes whereas the SMX mixer produces the highest ones. Nevertheless the mean diameter obtained with both SMV and SMX plus mixers are rather similar. As the SMX plus mixer produces the narrowest size distributions, it may be recommended for applications in turbulent flow.

These three mixers own different structures but the SMX and SMX plus ones are more similar. Nevertheless performances of the SMX plus mixer are closer to the SMV ones. The SMX mixer's crossbars are thicker than the SMX plus ones. This results in a lower porosity for the SMX plus mixer that is taken into consideration in the mean energy dissipated calculation. But it is possible that in addition of its influence on the energy dissipation, the crossbar's thickness plays a significant role in the break up phenomenon.

3.3.4. Correlation of experimental data

Models used to predict mean droplets diameter are generally based on Kolmogoroff's theory of turbulence (see Hinze, 1955, 1959). This theory assumes a flow field that should be both homogeneous and isotropic. Even if isotropy and homogeneity do not suit well to flows generated by static mixers the Kolmogoroff's theory is generally used to correlate maximum stable droplets diameters d_{max} as a function of mean energy dissipation rate per fluid mass unit as follows:

$$d_{max} = C_{11}\left(\frac{\sigma}{\rho_c}\right)^{0.6}\varepsilon_m^{-0.4} \tag{22}$$

where σ is the interfacial tension between both phases.

Moreover it is generally assumed that every characteristic diameter such as d_{50}, D_{32} or D_{43} characterizing droplets size distributions are proportional to maximum diameters as showed by Sprow (1967) for the case of liquid–liquid dispersion in stirred tank. Only few authors really examined this assumption for the case of static mixers (Berkman and Calabrese, 1988; Lemenand et al., 2001, 2003; Yamamoto et al., 2007).

For experimental data of the present study Sprow's relationship has been examined between d_{90} and D_{32} as d_{90} are reported with more confidence than d_{max} by the analytic method used for droplets size distributions analysis. Fig. 18 shows d_{90} as a function of D_{32} for experiments carried out with the SMV mixer. It shows that the relationship between d_{90} and D_{32} is well linear. The same result has been obtained with the two other mixers. Even the proportionality relationship of the D_{32} has not been checked toward the maximum diameter, results described here enables to work further with D_{32} as characteristic diameters are well proportional to each other as shown with d_{90} diameters.

In order to check that the turbulent flow field is comprised in the inertial subrange the Kolmogoroff's length scale η defined as follows as been calculated:

$$\eta = \left(\frac{\upsilon^3}{\varepsilon_m}\right)^{0.25} \tag{23}$$

where υ is the kinematics viscosity of the system that is here calculated for the continuous phase. In the flowrate range tested here Kolmogoroff's length scale ranges from 3 to 9 μm whereas Sauter mean diameters are comprised between 16 and 58 μm. This calculation enables to conclude that we are working in the inertial subrange. This enables to correlate experimental D_{32} to the mean energy dissipation rate per fluid mass unit in Fig. 17, the ratio σ/ρ_c being equal for each results series:

$$D_{32} = C_{12}\varepsilon_m^k \tag{24}$$

As shown on Fig. 17, k values range from −0.36 to −0.64. The k value obtained for the SMX mixer (k = −0.36) is rather closed to the value predicted by the Kolmogoroff's theory. The values obtained respectively for the SMX plus mixer (k = −0.52) and for the SMV mixer (k = −0.64) are smaller than the value predicted by the Kolmogoroff's theory. It may be assumed that flow fields generated by these mixers are less homogeneous and isotropic than the one generated by the SMX mixer. Such an assumption may be discussed on the basis of computational fluid dynamics analysis.

Results are also generally correlated in the literature in terms of dimensionless numbers. In this way Middleman (1974) proposed a correlation that takes into consideration the Reynolds and Weber numbers. The Weber number We_h is defined as follows in terms of continuous phase properties, hydraulic diameter and interstitial velocity:

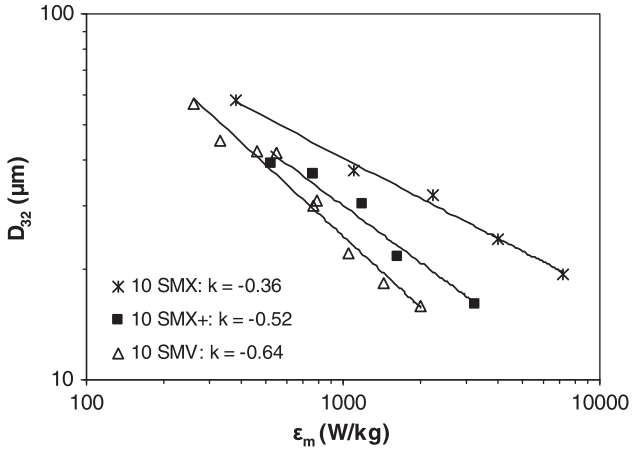

Fig. 17. Comparison of Sauter mean diameters obtained with the three designs as a function of the mean energy dissipated per fluid mass unit with n_e = 10.

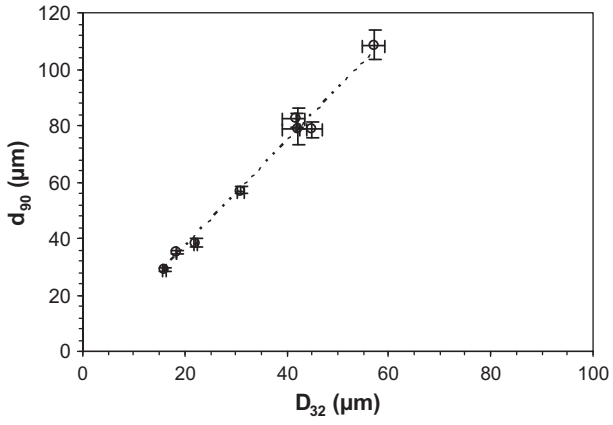

Fig. 18. d_{90} as a function of D_{32} for experimental results obtained with the SMV mixer with n_e = 10 and Φ = 0.25.

$$We_h = \frac{\rho_c V_0^2 D_h}{\sigma \varepsilon^2} \quad (25)$$

The correlation proposed by Middleman (1974) assumes the Kolmogoroff's theory of turbulence and is here written according to hydraulic numbers and continuous phase properties:

$$\frac{D_{32}}{D_h} = C_{13} We_h^{-0.6} f_h^{-0.4} \quad (26)$$

When pressure drops generated by the emulsion agree with a Blasius type correlation, the previous equation may be written in terms of Weber and Reynolds hydraulic numbers:

$$\frac{D_{32}}{D_h} = C_{14} We_h^{-0.6} Re_h^{0.1} \quad (27)$$

In order to correlate our experimental data through expression (27) the interfacial tension σ between both phases that is taken into account in the Weber number has been measured by the pendant drop method. Fig. 19 shows the evolution of interfacial tension value as a function of time. The first measurement depends on the drop formation time and is equal to 0.05 s. The interfacial tension decreases then from 12.0 mN/m to 10.5 mN/m in three seconds. Residence times of emulsion in static mixers resulting from total flowrates carried out are very low (from 0.10 to 0.03 s) and above all are lower than surfactant adsorption time at droplets interface. Experimental results are then modeled through Eq. (27) with an interfacial tension value of 12 mN/m which is the most relevant value considering the residence times involved in our experiments.

Fig. 20 shows that for the investigated flowrate range corresponding to the turbulent flow regime, experimental results fit well with Eq. (27). The deviation between constants values may be assigned to mixer's geometric characteristics except from the porosity and the hydraulic diameters that are still included in the Weber and Reynolds numbers. It is indeed likely that the design concept influences the local energy dissipation that governs the break up mechanisms and thus modifies the constant in the correlation.

3.3.5. Comparison to the literature

Correlations in terms of dimensionless numbers established by different authors who worked on liquid–liquid dispersion in static mixers are recapitulated in Table 8. When operating in turbulent flow regime the exponent attributed to the Weber number ranges from −0.5 to −0.859. But most of authors report values close to the one predicted by the Kolmogoroff's theory (−0.6). Moreover, only few authors report a dependency of the droplets mean diameter towards the Reynolds number. When it is the case the exponent attributed to this number is always lower than these attributed to the Weber number and its sign depends on the flow regime. In fact it is negative for the laminar flow regime and positive for the turbulent flow regime.

From Table 8 it appears that the parameter that mostly governs the break up phenomenon is the Weber number. In addition to hydrodynamic parameters, some authors take into account some physico-chemical parameters such as viscosity and density ratios, as well as the dispersed phase concentration. Some geometric parameters like the number of elements also influence mean droplets size as reported by Middleman (1974), Al Taweel and Walker (1983), El Hamouz et al. (1994) and Streiff et al. (1997). In a previous work dealing with liquid–liquid dispersion in SMX static mixer, we integrated this parameter with an exponent equal to −0.2 (Theron et al., 2010). Finally Sembira et al. (1984) reported the influence of the mixer's material on droplets size obtained through a comparison between SMV mixers made of stainless steel and Teflon. They explain this effect by a difference of relative wettability of both fluids towards the mixer's material.

There are only few comparisons between different mixers in the open literature. The only comparisons available (Al Taweel and Chen, 1996; Lemenand et al., 2003) have been presented in terms of generated interfacial area as a function of the mean energy dissipation rate per fluid mass unit. Experimental data of the present study are compared in Fig. 21 to data of the literature in terms of Sauter mean diameters as a function of energy dissipated. In fact Sauter mean diameters are more appropriate than interfacial area generated to well represent actual size ranges reached. In the same way, the energy dissipated obtained by multiplying the mean energy dissipation rate by the residence time in the mixer enables to best represent the actual energy cost of the operation.

For a relevant comparison mixers must be compared for same systems physical properties, which sometimes are missing. Interfacial tension is a physical parameter of major influence and is thus specified when possible. Streiff (1977) used different oils as dispersed phase including cyclohexane, what resulted in interfacial tension ranging from 24.7 to 46.0 mN/m. Al Taweel and Walker (1983) carried out experiments with the water/kerosene system, without precising the interfacial tension. The emulsions prepared by Berkman and Calabrese involved different oils what resulted in interfacial tension ranging from 31.8 to 41.6 mN/m. Lemenand et al. performed emulsification with the water/vaseline system resulting in a 20 mN/m interfacial tension.

From Fig. 21 it appears that Sulzer mixers represent higher energy costs than other designs, but enable to reach lower droplets size. This may be explained by the rather complex and close aspect

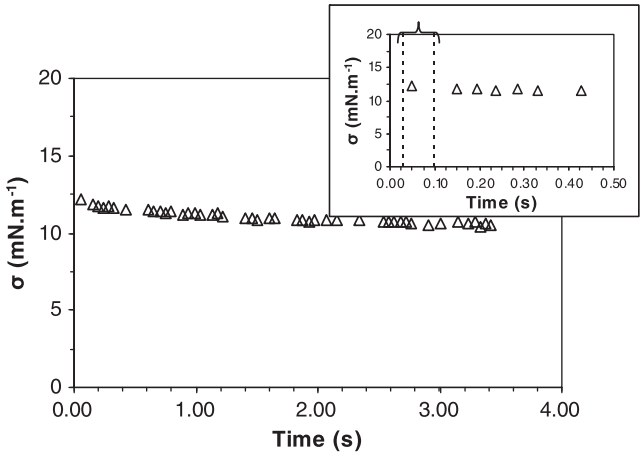

Fig. 19. Time evolution of Tween80 adsorption at water/cyclohexane interface.

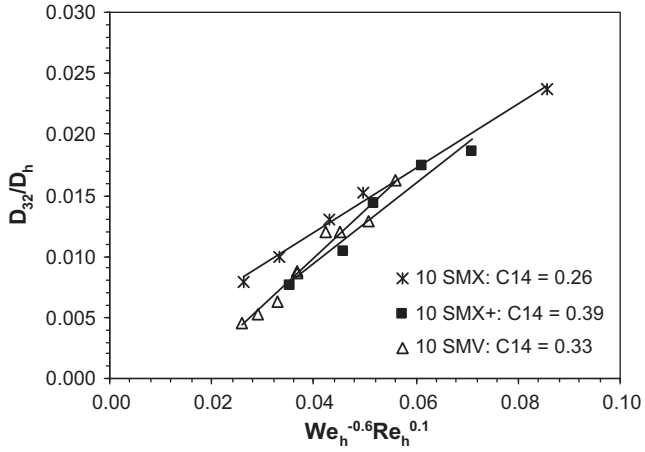

Fig. 20. Correlation of experimental data in terms of hydraulic Weber and Reynolds numbers.

Table 8
Correlations of the literature predicting mean diameters resulting from emulsification in static mixers.

Authors	Mixer's design	Characteristic diameter	Correlation	Flow regime
Middleman (1974)	Kenics	D	$\frac{D_{32}}{D} = KWe^{-0.6}\mathrm{Re}^{0.1}$	Turbulent
Streiff (1977)	SMV	D_h	$\frac{D_{32}}{D_h} = 0.21\,We_h^{-0.5}\mathrm{Re}_h^{0.15}$	Transient, turbulent
Chen and Libby (1978)	Kenics	D	$\frac{D_{32}}{D} = 1.14\,We^{-0.75}(\frac{\mu_d}{\mu_c})^{0.18}$	Turbulent
Matsumura et al. (1981)	Hi-mixer	D	$\frac{D_{32}}{D} = KWe_c^{-n} \quad n = 0.56 - 0.67$	Turbulent
Al Taweel and Walker (1983)	Lightnin	D_h	$\frac{D_{32}}{D_h} = K\,We^{-0.6}f^{-0.4}$	Turbulent
Haas (1987)	Kenics	D	$\frac{D_{43}}{D} = 1.2We^{-0.65}\mathrm{Re}^{-0.2}(\frac{\mu_d}{\mu_c})^{0.5}$	Laminar
Berkman and Calabrese (1988)	Kenics	D	$\frac{D_{32}}{D} = 0.49We^{-0.6}(1 + 1.38\,Vi(\frac{D_{32}}{D})^{0.33})^{0.6}$	Turbulent
Al Taweel and Chen (1996)	Woven screen		$D_{32} = 0.682(We_{jet}^{-0.859}\phi^{0.875})(\frac{b}{M})^{0.833}$	Turbulent
Streiff et al. (1997)	SMV, SMX, SMXL		$d = C_n(1 + K\phi)(\frac{(1+BVi)We_c}{2})^{0.6}(\frac{\sigma}{\rho_c})^{0.6}(\frac{\rho_c}{\rho_d})^{0.1}\varepsilon^{-0.4}$	
			$d_{\max} = 0.94(\frac{\sigma}{\rho_c})^{0.6}\varepsilon^{-0.4}$	
Legrand et al. (2001)	SMX	d_p	$\frac{D_{32}}{d_p} = 0.29We_p^{-0.2}\mathrm{Re}_p^{-0.16}$	Laminar, transient and turbulent
Lemenand et al. (2001, 2003, 2005)	HEV	D	$\frac{D_{32}}{D} = 0.57\,We^{-0.6}$	Turbulent
Das et al. (2005)	SMX	d_p	$\frac{d_{\max}}{d_p} = CWe_p^{-0.33}$	Laminar, transient
Rama Rao et al. (2007)	SMX	D	$\frac{D_{43}}{D} = K(1.5\phi(1 + \frac{\mu_d}{\mu_c}))^{0.5}$	Laminar
Hirschberg et al. (2009)	SMX plus		$d = C_n(1 + K\phi)(\frac{(1+BVi)We_c}{2})^{0.6}(\frac{\sigma}{\rho_c})^{0.6}(\frac{\rho_c}{\rho_d})^{0.1}\varepsilon^{-0.4}$	Turbulent
Theron et al. (2010)	SMX	D_{32}	$\frac{D_{32}}{D} = KWe^{-0.6}\mathrm{Re}^{0.1}n_e^{-0.2}$	Turbulent

of Sulzer mixers compared to the HEV mixer particularly and also to the Kenics and Lightnin mixers.

Droplets sizes obtained in the present study with the SMV mixer are lower than those reported by Streiff (1977). This discrepancy may be due to the interfacial tension difference between both studied systems. In fact σ is 2–4 times higher for the system studied by Streiff than σ of our system, what is rather important. In the Kolmogoroff's theory of turbulence the droplet size is correlated to the interfacial tension at the power of 0.6. So the droplet size is divided by 2 if σ is divided by 4. The discrepancy is here more important and might also be due to other parameters like mixer's geometrical parameters. In fact he used different SMV mixers with hydraulic diameter ranging from 2 to 64 mm whereas it is for our SMV mixer of 3.5 mm.

The comparison presented in Fig. 21 must then be considered cautiously as physico-chemical systems involved in these studies are different. As a conclusion it would be interesting to compare different geometries with a same system (dispersed phase, continuous phase, and surfactant).

4. Conclusion

Three Sulzer motionless mixers have been compared in terms of pressure drops and emulsification performances in turbulent flow regime. Pressure drop generated by a Newtonian single-phase flow in a SMX plus mixer are reduced of about 50% compared to the SMX mixer as predicted by CFD analysis by Hirschberg et al. (2009). Pressure drops resulting from the use of the SMV mixer are rather equal to those generated by the SMX plus mixer. Pressure drops produced by the three mixers have been successfully modeled through a Blasius type correlation.

Emulsification was performed in the three mixers with the water/Tween 80/cyclohexane system. The same correlation type as for single-phase flow has been used to model pressure drops generated by two-phase flow across the three mixers. In the flowrate range tested and for a dispersed phase concentration fixed to 25% in volume, Sauter mean diameters obtained ranged from 15 to 60 μm. The influence of the dispersed phase concentration was investigated for the SMX mixer, and when ranging from 10% to 60% in volume droplets size distributions obtained showed no coalescence phenomenon between 25% and 60%.

The representation of Sauter mean diameters as a function of mixer's number of elements enabled to point out that a good compromise between mean droplets diameter and pressure drop is reached at 10 elements for the three mixers. For a same total flowrate minimum droplets diameters are the same for the three mixers whereas maximum diameter obtained with the SMX mixer is lower than these obtained with the SMX plus and the SMV mixers. This phenomenon is surely due to the repartition and residence time of the fluid in the different eddy size zones of the mixers depending on their design. When comparing the three motionless mixers in terms of D_{32} as a function of mean energy dissipation rate per fluid mass unit, the best performances are reached with the SMV mixer.

Finally Sauter mean diameters were successfully correlated as a function of hydraulic Reynolds and Weber numbers, whatever the mixer design.

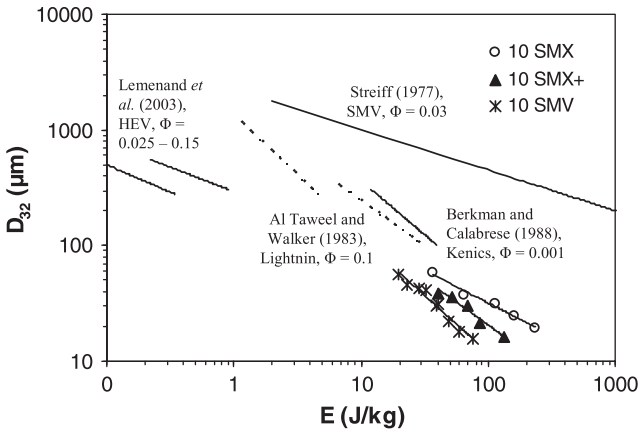

Fig. 21. Comparison of experimental data of the present study to results of the available literature.

Acknowledgments

The authors thank the Sulzer Chemtech Company and especially Dr. Philip Nising, Dr. Sebastian Hirschberg and Dr. Patrick Farquet for their technical support.

References

Alloca, P.T., 1982. Mixing efficiency of static mixing units in laminar flow. Fiber Producer 12, 19.

Al Taweel, A.M., Walker, L.D., 1983. Liquid dispersion in static in-line mixers. Can. Jour. Chem. Eng. 61, 527–533.

Al Taweel, A.M., Chen, C., 1996. A novel static mixer for the effective dispersion of immiscible liquids. Trans. IChemE 74, 445–450.

Berkman, P.D., Calabrese, R.V., 1988. Dispersion of viscous liquids by turbulent flow in a static mixer. AIChE J. 34, 602–609.

Bird, R.B., Stewart, W.E., Lightfoot, E.N., 1924. Transport Phenomena, 2nd ed. John Wiley and Sons, New York. Chapter 6, pp. 177–184.

Bohnet, M., Kalbitz, H., Nemeth, J., Pazmany, J., 1990. Improvement of forced convection heat transfer by using static mixers. In: Proc. Int. Act. Conf., INTC, Jerusalem, pp. 315–320.

Chen, S.J., Libby, D.R., 1978. Gas–liquid and liquid–liquid dispersions in a Kenics mixer. In: 71st Annual AIChE Meeting.

Cybulski, A., Werner, K., 1986. Static mixers-criteria for applications and selection. Int. Chem. Eng. 26, 171–180.

Das, P.K., Legrand, J., Morançais, P., Carnelle, G., 2005. Drop breakage model in static mixers at low and intermediate Reynolds number. Chem. Eng. Sci. 60, 231–238.

El Hamouz, A.M., Stewart, A.C., Davies, G.A., 1994. Kerosene/water dispersions produced by Lightnin ''in-line'' static mixer. IChemE Symp. Ser. 136, 457–464.

Fradette, L., Tanguy, P., Li, H.Z., Choplin, L., 2007. Liquid liquid viscous dispersions with a SMX static mixer. Trans. IChemE 85, 395–405.

Gingras, J.P., Fradette, L., Tanguy, P., Bousquet, J., 2007. Inline bitumen emulsification using static mixers. Ind. Eng. Chem. Res. 46, 2618–2627.

Grace, C.D., 1971. Static mixing' and heat transfer. Chem. Proc. Eng., 57–59.

Haas, P.A., 1987. Turbulent dispersion of aqueous drop in organic liquids. AIChE J. 33, 987–995.

Heywood, N.I., Viney, L.J., Stewart, I.W., 1984. Fluid Mixing II. The Institution of Chemical Engineers, Symposium Series, vol. 89, pp. 147–176.

Hinze, J.O., 1955. Fundamentals of the hydrodynamic mechanism of splitting in dispersion processes. AIChE J. 1, 289–295.

Hinze, J.O., 1959. Turbulence. Mc Graw-Hill, New York. 183 p.

Hirschberg, S., Koubek, R., Moser, F., Schock, J., 2009. An improvement of the Sulzer SMX static mixer significantly reducing the pressure drop. Chem. Eng. Res. Des. 87, 524–532.

Karoui, A., 1998. Caractérisation de l'hydrodynamique et du mélange dans les mélangeurs statiques Sulzer. Thèse de Doctorat.

Legrand, J., Morançais, P., Carnelle, J., 2001. Liquid liquid dispersion in an SMX Sulzer static mixer. Trans. IChemE 79, 949–956.

Lemenand, T., Zellouf, Y., Della Valle, D., Peerhossaini, H., 2001. Formation de gouttelettes dans un mélange turbulent de deux fluides immiscibles. 15ème Congrès Français de Mécanique, Nancy, pp. 494–499.

Lemenand, T., Della Valle, D., Zellouf, Y., Peerhossaini, H., 2003. Droplets formation in turbulent mixing of two immiscible fluids in a new type of static mixer. Int. J. Multphase Flow 29, 813–840.

Lemenand, T., Dupont, P., Della Valle, D., Peerhossaini, H., 2005. Turbulent mixing of two immiscible fluids. Trans. ASME 127, 1132–1139.

Li, H.Z., Fasol, C., Choplin, L., 1996. Hydrodynamics and heat transfer of rheologically complex fluids in a Sulzer SMX static mixer. Chem. Eng. Sci. 51, 1947–1955.

Li, H.Z., Fasol, C., Choplin, L., 1997. Pressure drop of Newtonian and non-Newtonian fluids across a Sulzer SMX static mixer. Trans. IChemE 75, 792–796.

Liu, S., Hrymak, A.N., Wood, P.E., 2005. Drop break up in an SMX static mixer in laminar flow. Can. J. Chem. Eng. 83, 793–807.

Matsumura, K., Morishima, Y., Masuda, K., Ikenaga, H., 1981. Some performance data of the Hi-mixer – An in-line mixer. Chem. Ingenieur. Technol. 53, 51–52.

Middleman, S., 1974. Drop size distributions produced by turbulent pipe flow of immiscible fluids through a static mixer. Ind. Eng. Chem., Process. Des. Develop. 13, 78–83.

Mutsakis, M., Streiff, F., Schneider, G., 1986. Advances in static mixing technology. Chem. Eng. Prog., 42–48.

Myers, K.J., Bakker, A., Ryan, D., 1997. Avoid agitation by selecting static mixers. Chem. Eng. Prog., 28–38.

Pahl, M.H., Muschkelnautz, E., 1979. Einsatz und anslegung statischer mischer. Chem. Ingenieur Technol. 51, 347–364.

Pahl, M.H., Muschkelnautz, E., 1980. Statische mischer und ihre anwendung. Chem. Ingenieur Technol. 52, 285–291.

Pahl, M.H., Muschkelnautz, E., 1982. Static mixers and their applications. Int. J. Chem. Eng. 22, 197–205.

Rama Rao, N.V., Baird, M.H.I., Hrymak, A.N., Wood, P.E., 2007. Dispersion of high-viscosity liquid liquid systems by flow through SMX static mixer elements. Chem. Eng. Sci. 62, 6885–6896.

Sembira, A.N., Merchuck, J.C., Wolf, D., 1984. Characteristics of a motionless mixer for dispersion of immiscible fluids – I. A modified electroresistivity probe technique. Chem. Eng. Sci. 41, 445–455.

Shah, N.F., Kale, D.D., 1991. Pressure drop for laminar flow of non-Newtonian fluids in static mixers. Chem. Eng. Sci. 46, 2159–2161.

Shah, N.F., Kale, D.D., 1992. Pressure drop for laminar flow of viscoelastic fluids in static mixers. Chem. Eng. Sci. 47, 2097–2100.

Sprow, F.B., 1967. Distribution of drop sizes produced in turbulent liquid–liquid dispersion. Chem. Eng. Sci. 22, 435–442.

Streiff, F.A., 1977. In-line dispersion and mass transfer using static mixing equipment. Sulzer Techn. Rev. 108, 113.

Streiff, F.A., Mathys, P., Fischer, T.U., 1997. New fundamentals for liquid liquid dispersion using static mixers. Récents Prog. Génie Procédés 11, 307–314.

Streiff, F.A., Jaffer, S., Schneider, G., 1999. The design and application of static mixer technology. In: 3rd International Symposium on Mixing in Industrial Processes, Osaka, Japan, pp. 107–114.

Thakur, R.K., Vial, K.D.P., Nauman, E.B., Djelveh, G., 2003. Static mixers in the process industries – a review. Trans. IChemE 81, 787–826.

Theron, F., Le Sauze, N., Ricard, A., 2010. Turbulent liquid–liquid dispersion in Sulzer SMX mixer. Ind. Eng. Chem. Res. 49, 623–632.

Yamamoto, T., Kawasaki, H., Kumazawa, H., 2007. Relationship between the dispersed droplet diameter and the mean power input for emulsification in three different types of motionless mixers. J. Chem. Eng. Jpn. 40, 673–678.

Yang, H.C., Park, S.K., 2004. Pressure drop in motionless mixers. KSME Int. J. 18, 526–532.